THE ASTROPHYSICAL JOURNAL, 553:886–896, 2001 June 1

THE TYPE Ic SN 1990B IN NGC 4568

ALEJANDRO CLOCCHIATTI,[1] NICHOLAS B. SUNTZEFF,[2] MARK M. PHILLIPS,[3] ALEXEI V. FILIPPENKO,[4] MASSIMO TURATTO,[5] STEFANO BENETTI,[5] ENRICO CAPPELLARO,[5] ROBERTO AVILÉS,[6] RICARDO COVARRUBIAS,[2] K. DEGIOIA-EASTWOOD,[7] MARK DICKINSON,[8] CHRISTIAN GOUIFFES,[5] PURAGRA GUHATHAKURTA,[9] MARIO HAMUY,[10] STEVE R. HEATHCOTE,[2] BRUNO LEIBUNDGUT,[11] THOMAS MATHESON,[4] MAURICIO NAVARRETE,[3] M. PEREZ,[2] ANDREW PHILLIPS,[12] ANTONELLO PIEMONTE,[1] MARÍA T. RUIZ,[13] JOSEPH C. SHIELDS,[14] CHRIS SMITH,[2] HYRON SPINRAD,[4] CONRAD R. STURCH,[15] J. ANTHONY TYSON,[16] AND LISA WELLS[10]

Received 2000 March 14; accepted 2001 January 16

ABSTRACT

We present a study of the Type Ic supernova (SN) 1990B that includes most of the observations obtained from around the world. The combined data set comprises 84 $BV(RI)_c$ photometric points spanning approximately 360 days after maximum light and 14 spectra from 5 up to ~150 days after maximum light. In contrast to other Type Ic SNe, SN 1990B did not display a weak but distinct He I λ5876 line indicating that its He content was smaller or that the He layers were rather effectively shielded from the radioactive matter in the ejecta. The behavior of the Na I D line, however, suggests that He I λ5876 was blended with it. SN 1990B appeared on a sharply varying background that complicates the usual techniques of digital photometry. In order to do unbiased photometry, we modeled and subtracted the background of each image with the SN using images of NGC 4568 taken ~2500 days after the explosion, when SN 1990B had faded beyond detection. We compare the performance of standard point-spread function fitting photometry of the SN in the images with and without the background of the parent galaxy and find the results to differ systematically at late times. The photometry done on the images with the background light of NGC 4568 subtracted shows the light curves of SN 1990B to be of the slow Type Ic variety, with a slope steeper than that of the Type Ib SN 1983N or the Type II transition (Type IIb) SN 1993J but slower than that of the Type Ic SN 1994I. We estimate the reddening by foreground matter in the Galaxy and NGC 4568 and compute $BV(RI)_c$ light curves spanning ~110 days after maximum light.

Subject headings: supernovae: general — supernovae: individual (SN 1990B)

1. INTRODUCTION

Supernova (SN) 1990B was discovered by the Berkeley Automated Supernova Search (Perlmutter & Pennypacker 1990) on five unfiltered CCD images taken during 1990 January 21.45–21.51 at a projected position close to the center of the SA galaxy NGC 4568 (see Figs. 1 and 2). Reports of optical spectra were soon announced, indicating that the SN was of Type I (Dopita & Ryder 1990), Type Ib (Kirshner & Leibundgut 1990), and helium-weak Type Ib (i.e., Type Ic; Filippenko, Spinrad, & Dickinson 1990). The reports also emphasized the red character of the spectrum and the presence of strong narrow lines of interstellar origin, consistent with Na I D at the velocity of the parent galaxy. Cerro Tololo Inter-American Observatory preliminary photometry and spectrophotometry (Suntzeff et al. 1990) and the nondetection of the SN in two long exposures with the *IUE* long-wavelength camera (Panagia et al. 1990) confirmed the red character of the SN. Preliminary estimates of the foreground interstellar reddening ranged from $E(B-V) = 0.9$ mag (Suntzeff et al. 1990) to 1.5 mag (Benetti, Cappellaro, & Turatto 1990). The SN was also detected at radio wavelengths starting as soon as 3 weeks after discovery (Sramek, Weiler, & Panagia 1990).

Extensive observational follow-up of SN 1990B continued for up to a year after discovery. A comprehensive study of the radio emission from SN 1990B was presented by Van Dyk et al. (1993). A preliminary study of the optical and near-infrared photometry and spectroscopy was given by Clocchiatti et al. (2000b). In this paper we analyze the complete data sets of the Cerro Tololo Inter-American Observatory (CTIO), European Southern Observatory (ESO), Osservatorio Astrofisico di Asiago (OAA), Lick Observatory, Kitt Peak National Observatory (KPNO), and Fred L. Whipple Observatory (FLWO), which amount to 14 spectra with good time sampling spanning ~150 days after maximum and 84 photometric points in $BV(RI)_c$ that

[1] Departamento de Astronomía y Astrofísica, Pontificia Universidad Católica, Casilla 306, Santiago 22, Chile; aclocchiatti@astro.puc.cl.
[2] Cerro Tololo Inter-American Observatory, National Optical Astronomy Observatories, Casilla 603, La Serena, Chile; nsuntzeff@noao.edu.
[3] Carnegie Institution of Washington, Las Campanas Observatory, Casilla 601, La Serena, Chile; mmp@lco.cl.
[4] Department of Astronomy, University of California, Berkeley, Berkeley, CA 94720.
[5] Osservatorio Astronomico di Padova, Vicolo dell'Osservatorio 5, I-35122 Padova, Italy.
[6] Departamento de Física, Universidad de Chile, Casilla 487-3, Santiago, Chile.
[7] Department of Physics and Astronomy, Northern Arizona University, Box 6010, Flagstaff, AZ 86011-6010.
[8] STScI, 3700 San Martin Drive, Baltimore, MD 21218.
[9] UCO/Lick Observatory, University of California, Santa Cruz, CA 95064.
[10] University of Arizona, Steward Observatory, Tucson, AZ 85721.
[11] European Southern Observatory, Karl-Schwarzschild-Strasse 2, D-85748 Garching bei München, Germany.
[12] Lick Observatory, University of California, 1156 High Street, Santa Cruz, CA 95064.
[13] Departamento de Astronomía, Universidad de Chile, Casilla 36-D, Santiago, Chile.
[14] Ohio University, Department of Physics and Astronomy, Clippinger Research Laboratories 251B, Athens, OH 45701-2979.
[15] Computer Sciences Corporation, Space Telescope Science Institute, Homewood Campus, Baltimore, MD 21218.
[16] Bell Laboratories, Lucent Technologies, Room 1D432, 700 Mountain Avenue, Murray Hill, NJ 07974.

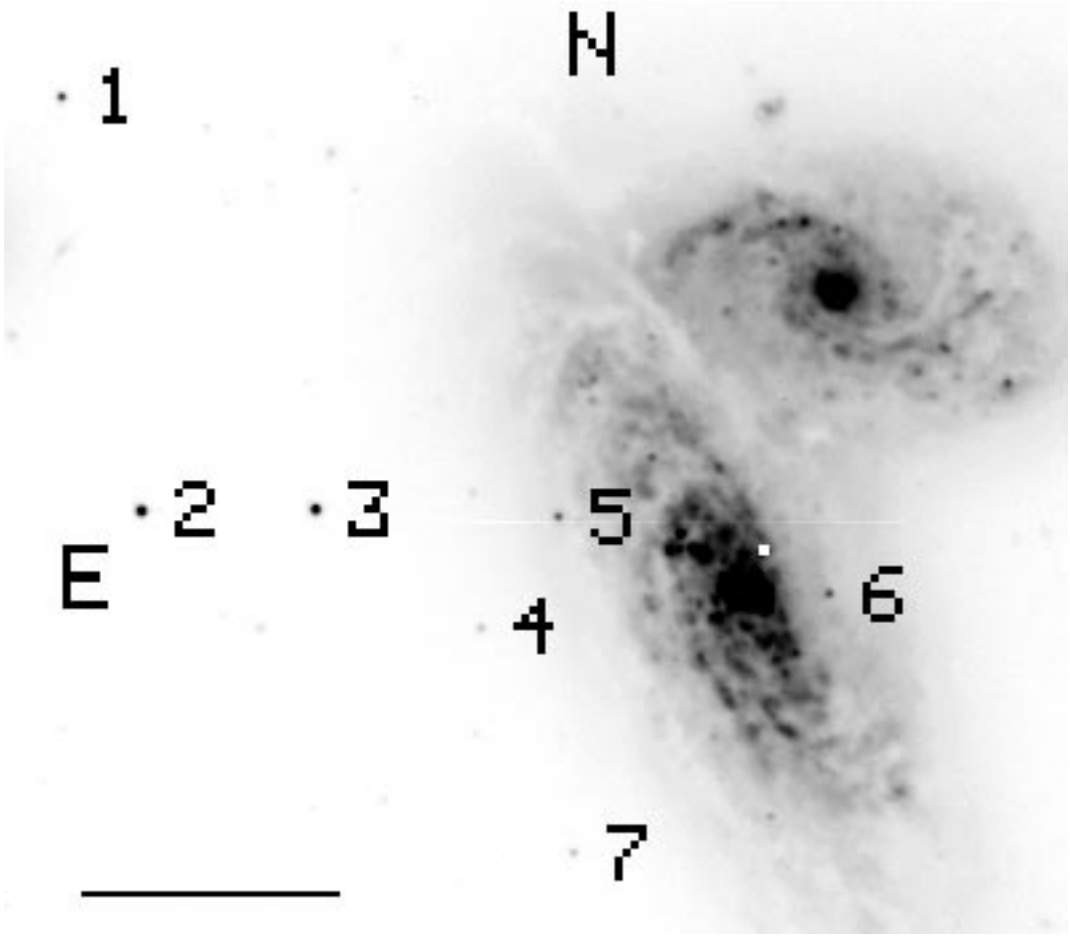

FIG. 1.—Chart of the region of SN 1990B. The sequence of local standard stars used to calibrate the brightness of the SN is labeled by numbers positioned toward the northwest of the referenced stars. The position of the SN is given by a white square dot toward the northwest of the center of NGC 4568 (close to the line joining stars 5 and 6). The horizontal bar on the lower left corner represents 1′.

sample the light curves for more than 360 days after maximum.

Stripped envelope core-collapse SNe (SESNe), among which the Type Ib/c are included, are still one of the open frontiers for basic observational work on SNe. Since they cannot be used to estimate distances, like Type Ia or Type II SNe, their follow-up is routinely neglected unless they are bright or peculiar in some respect. Type Ic SNe were first recognized as a variant of the Type Ib ones (Wheeler et al. 1987). They not only lack the strong Si II λ6355 line that Type Ia SNe show near maximum light, but they also lack the strong He I lines that Type Ib display at early times. Owing to this fact, they have also been called "He–poor" Type Ib SNe (Filippenko, Porter, & Sargent 1990). The evidence accumulated has been gradually showing that Type Ic SNe are a very heterogeneous group (Clocchiatti & Wheeler 1997a, 1997b). After a peak in activity during 1993–1996, which resulted mainly from the impact of the bright and well-observed SNe 1993J and 1994I, the field of these "exotic" SNe entered a time of slower productivity, with the notable exception of the studies of SN 1998bw probably associated with GRB 980425. A review of the observational material prior to SN 1998bw is given by Filippenko (1997). Some SESNe of the Type Ic, however, were well-observed during the 1990s, and their records have not yet been made public. The present study of SN 1990B is a step toward this goal.

In § 2 we present the spectroscopic observations and briefly discuss the classification issues and the evidence for light chemical elements in the outer layers of SN 1990B. In § 3 we present the photometric observations and discuss the steps taken to do photometry. In § 4 we discuss the light curves and present $BV(RI)_c$ light curves, which are suitable to compare with SN theoretical models. Finally, in § 5 we discuss and summarize our results.

2. SPECTRA

We collected 14 spectra, which in many cases are the product of multiple exposures at different wavelength settings. Image processing and calibration followed the typical procedures. The two-dimensional CCD spectra were divided by normalized flat-field images built from several exposures of the dome, illuminated by light sources that provide good signal-to-noise ratio (S/N) in all the spectral range. Spectra of the SN were extracted and sky-subtracted, with special care taken in fitting the background underneath the SN profile, since SN 1990B appeared superposed on a complicated background (see Figs. 1 and 2). The spectra were linearized in wavelength using the line spectra of different gas mixtures (typically He-Ar, or He-Ne-Ar), corrected for atmospheric extinction using the mean extinction curve for the different observatories, and calibrated in flux using the sensitivity curve for the night, obtained from different spectrophotometric standards. In some cases, hot

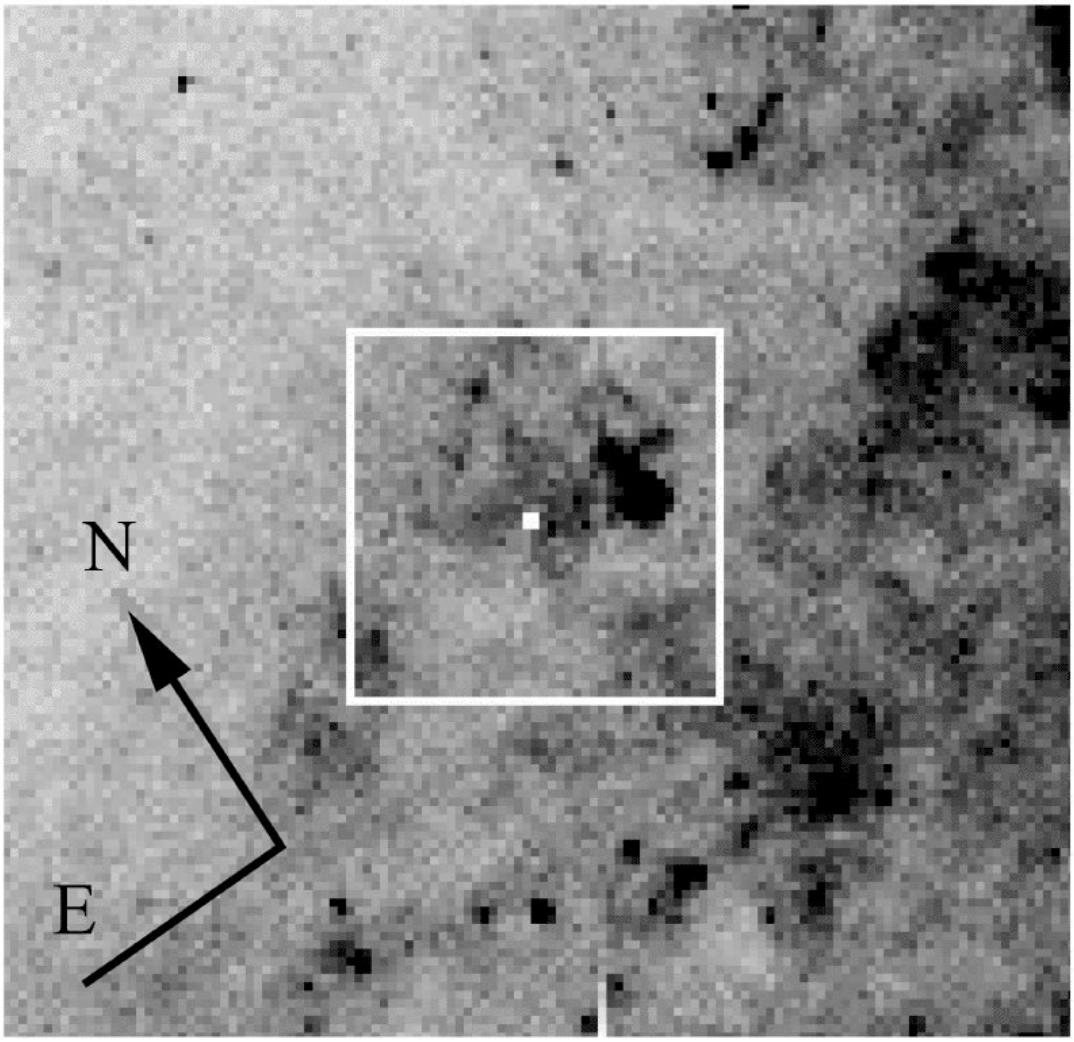

FIG. 2.—*HST* image of the region of SN 1990B. The image was taken through filter F606W. Exposure time was 80 s. The position of the SN is marked by a filled square. The larger square box centered on the SN has 1″ sides.

stars at a similar air mass and position in the sky were observed with the same spectrograph setting, to build response functions for the telluric atmospheric absorption bands, and attempts were made to remove these bands from the SN spectra. More detail on the spectroscopic observations is given in Table 1.

The spectral sequence of the SN during the photospheric and nebular phases is plotted in Figures 3 and 4, respectively. As had been remarked in the earlier reports (see § 1), the spectra show strong interstellar Na I D lines in the rest frame of the parent galaxy, revealing that the SN was heavily reddened. The velocity of NGC 4568, obtained from the average of the superposed Na I D and narrow Hα lines in the highest quality SN spectra, is 2230 ± 50 km s^{-1}, in good agreement with the results of de Vaucouleurs et al. (1991). There is, in addition, a weak narrow line at the rest wavelength of Galactic Na I D, indicating that SN 1990B also suffered a modest amount of reddening from interstellar matter associated with the Milky Way (see § 3). The equivalent widths of the Na I D lines in NGC 4568 and the Milky Way, measured on the spectra with the best resolution and S/N, are 7.5 ± 0.2 and 1.3 ± 0.2 Å, respectively.

Although SN 1990B was later recognized as a Type Ic SN, earlier reports in the IAU circulars (see § 1) called it a Type Ib SN. We feel it is important to clear the record. With this purpose, we have included Figure 5, showing a comparison of the spectrum of SN 1990B with those of the Type Ic SNe 1987M (Filippenko, Porter, & Sargent 1990) and 1994I (Filippenko et al. 1995; Clocchiatti et al. 1996). Figure 5 reveals that there are no major differences between the spectra of typical Type Ic SNe 1994I or 1987M and that of SN 1990B, although there are some minor ones. The spectrum of SN 1990B shows deeper and narrower line cores at a given phase and this, together with the absence of Si II λ6355, suggests a lower photospheric temperature for SN 1990B. In general the spectrum of SN 1990B resembles the spectra that the other two SNe would show at later phases.

The evidence for helium in SN 1990B is also different than that for SNe 1987M and 1994I. Starting a few days after maximum, SNe 1987M and 1994I displayed a weak He I λ5876 at very high velocity (Clocchiatti et al. 1996). The He I line appears on the blue shoulder of the Na I D line. In the case of SN 1994I, after a few days the two lines merge, while they evolve as separate troughs in the case of

TABLE 1

SPECTROSCOPIC OBSERVATIONS OF SN 1990B

UT Date (1990)	JD[a]	Phase[b]	Observatory and Telescope	Range (Å)	Observer
Jan 23.30.....	7914.80	4.80	Lick 3.0 m	4170–8078	H. Spinrad
Jan 26.32.....	7917.82	7.82	CTIO 1.5 m	3872–8547	M. T. Ruiz
Feb 04.04	7926.54	16.54	OAA 1.82 m	4090–7956	E. Cappellaro
Feb 06.30	7928.80	18.80	CTIO 1.5 m	3855–10320	M. Hamuy
Feb 11.50	7934.00	24.00	Palomar 5.0 m	3813–9727	A. Filippenko
Feb 16.33	7938.83	28.83	ESO NTT	3800–8622	C. Gouiffes
Feb 27.00	7949.50	39.50	Lick 3.0	4170–8138	H. Spinrad
Mar 04.34.....	7954.84	44.84	CTIO 4.0 m	3672–8965	M. M. Phillips
Mar 08.20.....	7958.70	48.70	ESO NTT	4402–11170	C. Gouiffes
Mar 25.50.....	7976.00	66.00	Lick 3.0 m	3919–9727	A. Filippenko
Apr 01.50	7983.00	73.00	Lick 3.0 m	3919–9727	A. Filippenko
Apr 19.17	8000.67	90.67	ESO 3.6 m	3806–9226	C. Gouiffes
Apr 30.50	8012.00	102.00	Lick 3.0 m	3971–9756	A. Filippenko
Jun 15.50	8058.00	148.00	Lick 3.0 m	6660–9805	A. Filippenko

[a] JD − 2,440,000.

[b] Days since *B* maximum on JD: 2,447,910 (i.e., UT 1990 January 18.5).

SN 1987M. He I λ5876 does not appear as a distinct line in SN 1990B. From this point of view, the spectrum of SN 1990B resembles more that of SN 1983V (Clocchiatti et al. 1997). The latter does not show a clear He I line, but there are signs of it merging with the blue side of the Na I D line. As a result, Na I D displays an anomalous shift to the blue in time, while the rest of the lines evolve as usual, drifting to smaller velocities with time. Evidence for He in SN 1990B appears, in principle, less compelling than in SN 1983V since, as shown in Figure 6, the broad feature at the position of Na I D does not display the characteristic shift to the blue with time.

There are signs, however, that do point at the presence of He I λ5876 in SN 1990B. First, the Na I D line of SN 1990B appears to be as wide as that of SN 1994I, while the Fe II and O I lines are narrower. This suggests that by 4.8 days after *B* maximum the He I λ5876 has already merged with

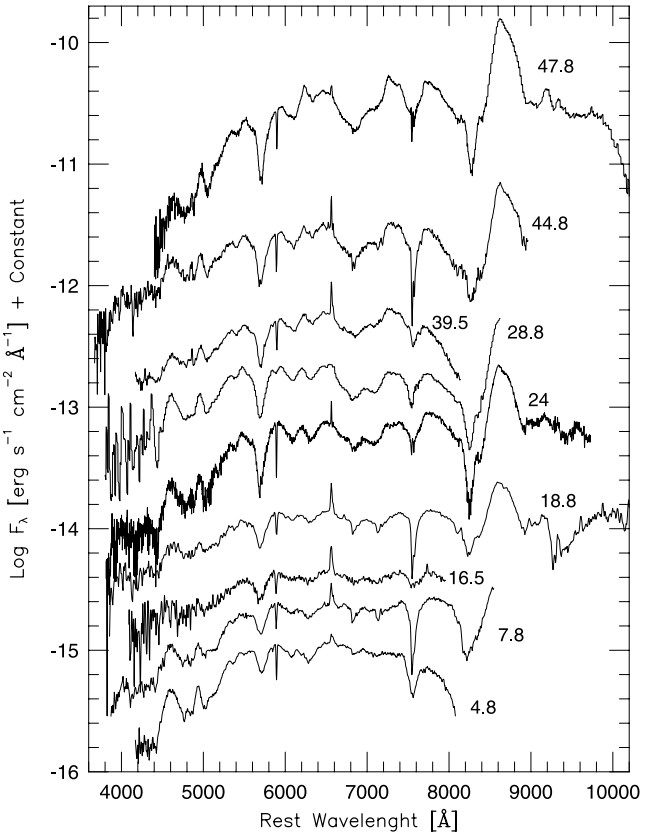

FIG. 3.—Spectroscopic evolution of SN 1990B from the photospheric up to the early nebular phases. The wavelength scale has been corrected for the velocity of the parent galaxy (2230 km s^{-1}; see § 2). The labels close to each line give the phase of the spectrum in days from *B* maximum.

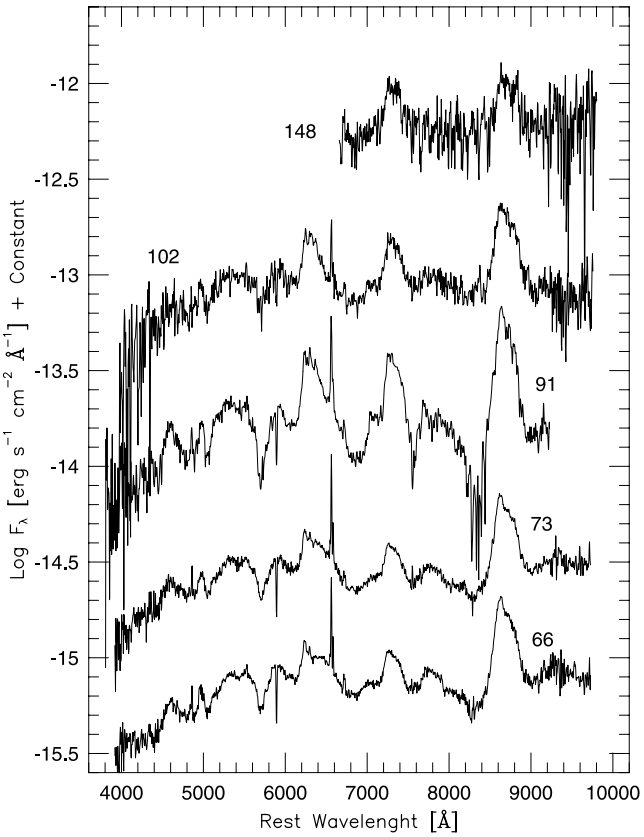

FIG. 4.—Same as Fig. 3, but the spectra of the nebular and late nebular phases are displayed.

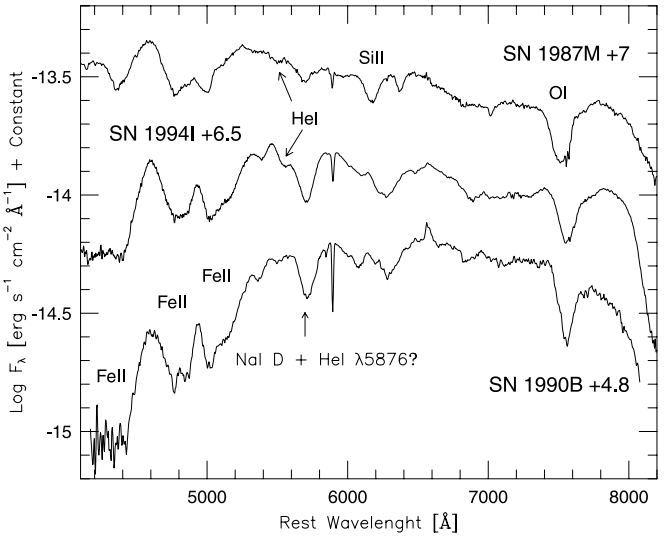

FIG. 5.—Comparison of the spectrum of SN 1990B with those of the Type Ic SNe 1987M (Filippenko, Porter, & Sargent 1990) and 1994I (Clocchiatti et al. 1996). The wavelength scales of the spectra have been corrected for the redshift of the parent galaxies. The main features of Fe II, Na I D, He I, Si II, and O I, are indicated.

Na I D in SN 1990B. Second, the velocity contrast between Na I D and Fe II λ5169 is very large (see Fig. 6). In other Type Ic SNe, Fe II λ5169 and Na I D tend to be at a similar velocity (with Fe II being faster than Na I D at early times)

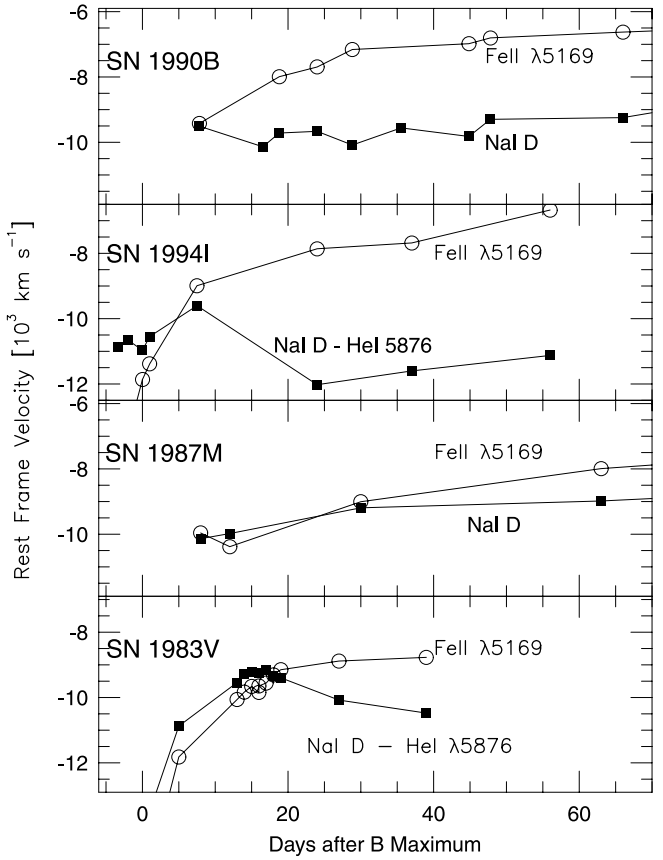

FIG. 6.—Rest-frame expansion velocity of the Fe II λ5169 and Na I D lines for SN 1990B (*top panel*), SN 1994I (*second panel from top*), SN 1987M (*third panel from top*), and SN 1983V (*bottom panel*).

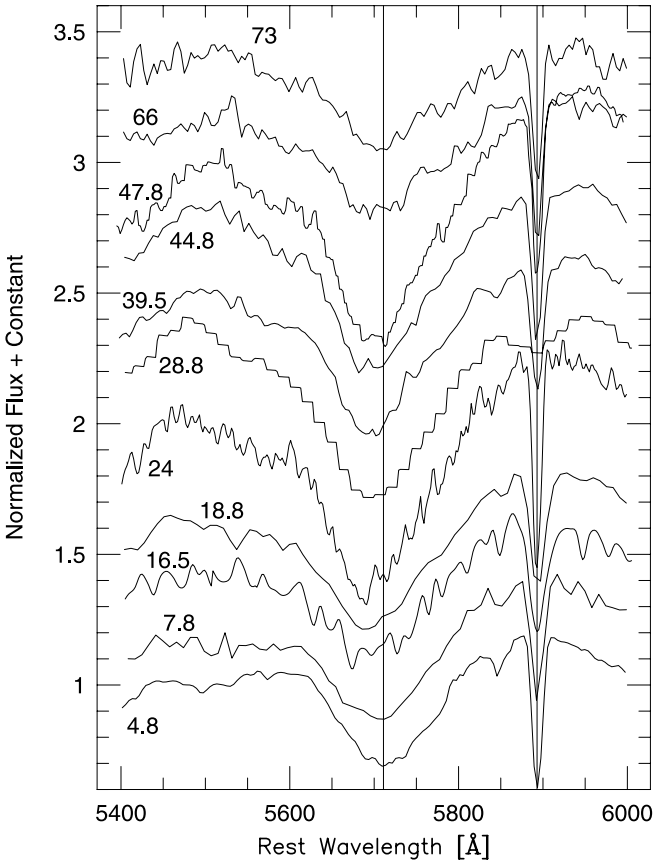

FIG. 7.—Evolution of the Na I D and He I λ5876 blend in SN 1990B (see § 2). The spectra have been adjusted to the rest frame of the parent galaxy, and additional small shifts have been applied, consistent with the resolution, to align the narrow Na I D lines of interstellar origin. All spectra were normalized by the flux at 5500 Å, and additional vertical shifts for clarity were added. The numbers close to the lines give the estimated phase in days since *B* maximum.

when the He I λ5876 line is not merged with Na I D. This is shown by the cases of SNe 1983V and 1994I before the merging of He I λ5876 and Na I D and by the case of SN 1987M, where the merging never occurs (see Fig. 6). Third, there is a subtle distortion that shifts to the blue the core of the Na I D line, without significantly changing the centering of the broad part of the feature (i.e., without significantly altering the velocity plotted in Fig. 6). The distortions are more clearly seen in Figure 7, where an expanded view of ~600 Å around He I λ5876 is shown. These facts suggest that He I, although very weak, was present in the spectrum of SN 1990B and that the merger of He I and Na I D happened close to maximum light, before the first spectrum was taken. If the distortions on the blue side of Na I D are caused by the merging of a He I λ5876 feature (as they were in SN 1994I), then the mean velocity of the He layer would have been $\sim 6500 \pm 2600$ km s^{-1}. In the absence of earlier optical spectra or infrared spectra near maximum light, however, the presence of He I in SN 1990B will remain controversial.

3. CCD PHOTOMETRY

We collected many CCD images of SN 1990B taken at different observatories. A description of the dates, telescopes used, observers, and other relevant information is

given together with the photometry in Table 3. We select and present in this paper only the images taken through standard Johnson *B* and *V* (Johnson 1955) and Cousins *R* and *I* (Cousins 1976a, 1976b, 1978). The images were reduced following the standard procedures. The CCD pedestal was corrected using the overscan regions, and any remaining two-dimensional pattern was removed using bias images, when necessary. Correction for dark current was applied, if required, when calibrating images were available. Pixel-to-pixel sensitivity variations were removed using median dome and/or sky flat-field images.

Several of the nights when the SN was observed were photometric. Using observations of standard stars from the lists of Graham (1982), Menzies et al. (1989), and Landolt (1992), zero points, color terms, and extinction coefficients were obtained, which allowed calibration of a sequence of local standard stars indicated in Figure 1. The values given in Table 2 are the average of two photometric nights for stars 5 and 6 and seven photometric nights for the others.

SN 1990B appeared on a complicated background. It is on a spiral arm and near bright H II regions, which make the sky underneath the SN bright and strongly nonuniform at angular scales comparable to the typical width of the point-spread function (PSF) of ground-based observations. A *Hubble Space Telescope* (*HST*) image of the area taken on 1995 February 4 (see Fig. 2) shows in great detail the strong brightness gradients of the region and, in addition, makes it clear that the SN was close to a minimum in the brightness distribution. We recognized that configurations like this complicate both aperture and PSF fitting photometry and decided to use our extensive database of images to test the performance of different photometric techniques in this case of a variable light source on a bright background with sharp gradients.

3.1. *Standard PSF Fitting Photometry*

For a subset of the images, which includes all the images taken from OAA, ESO, and some of the epochs taken from CTIO, we used ROMAFOT, a photometric package in MIDAS,[17] which allows simultaneous fitting of the PSF and sky, including a linear gradient in the latter. We built the mean PSF of the frames from isolated stars with good S/N and fitted this PSF to the stars in the local photometric sequence around NGC 4568 and to the image of the SN on top of the luminous background to obtain the instrumental magnitudes. We subtracted the fitted PSFs and carefully checked that, in particular, the residual of the SN after subtraction of the fitted PSF resembled the image of the galaxy without the SN. In addition, for a subset of these images and a few of those taken from CTIO, we computed instrumental magnitudes using the PSF fitting tasks in IRAF[18] package DAOPHOT, which allows for the simultaneous fitting of a constant sky underneath the PSF.

We transformed the instrumental magnitudes to the standard system using the calibration of the local sequence given in Table 2. The color terms for the CCDs and instruments used are small, but we nevertheless applied color-term corrections in those cases when the information was available.

Photometry done with IRAF's DAOPHOT or MIDAS's ROMAFOT tended to provide similar results, as if the presence of a gradient for the background underneath the SN were not a critical element. The magnitudes of SN 1990B obtained with DAOPHOT or ROMAFOT were used to study the results of different photometric techniques applied to this SN (see the discussion in § 3.2) but are not given in this paper.

3.2. *Background Subtraction*

In our preferred photometric approach, we subtracted the background of the parent galaxy using well-sampled and good S/N images of the region observed at a very late epoch. These very late time images, which we will call in what follows the "templates," were taken with the 0.91 m telescope at CTIO between January and February of 1997. The long separation between maximum and the templates (more than 2500 days) ensures that the SN had already faded beyond detection.

We used the image-matching algorithms described by Phillips & Davis (1995), which have been incorporated in IRAF V2.11 in the package IMMATCH, proceeding in detail as follows: (1) We shifted, rotated, and scaled the templates, so that the centers of the stars were in coincidence with those of the image with the SN; (2) we found the difference kernel that, when convolved with the image of the narrowest PSF (usually this is the template), would degrade it to match the PSF of the other image and convolved the image with better seeing with that kernel; (3) we found the linear transformation in intensities to make the template match the intensities of the image with the SN and applied that transformation to the template; and (4) we subtracted the region around the SN of the transformed

[17] The Munich Image Data and Analysis System (MIDAS) is developed and maintained by the European Southern Observatory.

[18] The Image Reduction and Analysis Facility (IRAF) is maintained and distributed by the Association of Universities for Research in Astronomy, Inc., under a cooperative agreement with the National Science Foundation.

TABLE 2

LOCAL STANDARD SEQUENCE

ID	*B*	*V*	R_c	I_c	$B-V$
1.....	20.42 ± 0.02	18.72 ± 0.02	17.41 ± 0.02	15.81 ± 0.02	1.69 ± 0.03
2.....	18.53 ± 0.02	17.63 ± 0.02	17.06 ± 0.02	16.56 ± 0.02	0.90 ± 0.03
3.....	18.68 ± 0.02	17.83 ± 0.02	17.30 ± 0.02	16.84 ± 0.02	0.84 ± 0.03
4.....	22.11 ± 0.15	20.16 ± 0.03	19.05 ± 0.02	17.63 ± 0.02	1.95 ± 0.15
5.....	20.19 ± 0.11	19.07 ± 0.07	18.44 ± 0.10	17.81 ± 0.10	1.12 ± 0.13
6.....	19.83 ± 0.09	19.36 ± 0.05	18.97 ± 0.08	18.58 ± 0.10	0.47 ± 0.10
7.....	21.56 ± 0.08	20.17 ± 0.03	18.95 ± 0.02	17.55 ± 0.02	1.39 ± 0.08

template from the image with the SN. After this procedure we found that the background of the parent galaxy near the SN had been mostly removed and that the sky underneath the SN was flatter than in the original image.

For this set of images, which have been background-subtracted, we did relative photometry of the SN using the tasks of the package DAOPHOT in IRAF. We built a mean PSF for each frame from the profiles of the stars in the field and found the instrumental magnitudes of the local sequence of standards and the SN by fitting this PSF function.

The instrumental magnitudes of the SN were transformed to the standard system using the magnitudes of the local standard sequence given in Table 2. The color terms for all the combinations of CCDs and instruments used is small, but we nevertheless applied the color-term corrections in all cases when the information was available. The magnitudes of the SN, calibrated in this way, are given in Table 3.

The two different photometric techniques described gave overall consistent results, although an interesting trend with potentially damaging consequences for SN studies was recognized. Close to maximum light, when the S/N under the PSF of the SN is high and there is a good contrast between the SN and the background, the results are consistent within the photometric uncertainty. However, as the SN gets dimmer, the result of not subtracting the background is to overestimate systematically the brightness of the SN. At late times, the background contamination can be more than a factor of 10 larger than the formal photometric errors. This effect sets a strong note of caution for the interpretation of the late-time light curves of SNe measured with CCDs, when the photometry is done on images that have the background of the parent galaxy. The slope of the late-time light curves of SNe obtained without subtracting the background should be taken with care when compared with theoretical models because they will be, typically, lower

TABLE 3

PHOTOMETRY OF SN 1990B WITH BACKGROUND SUBTRACTION

UT Date (1990)	JD[a]	Telescope[b]	B	V	R_c	I_c	Observer[c]
Jan 24.33	7915.83	T-.9	17.84 ± 0.02	15.97 ± 0.02	15.09 ± 0.02	...	MP
Jan 25.37	7916.87	T-.9	18.03 ± 0.03	16.10 ± 0.02	15.22 ± 0.02	14.50 ± 0.02	LW
Jan 28.35	7919.85	T-4	...	16.29 ± 0.05	15.42 ± 0.03	...	JT/PG
Jan 28.37	7919.87	T-.9	18.25 ± 0.03	16.40 ± 0.02	...	...	CS
Jan 29.30	7920.80	T-4	...	16.43 ± 0.02	15.55 ± 0.02	14.80 ± 0.02	JT/PG
Jan 29.30	7920.80	T-.9	...	...	15.52 ± 0.02	...	CS
Jan 30.32	7921.82	T-.9	18.39 ± 0.02	16.56 ± 0.02	15.62 ± 0.02	...	CS
Feb 02.33	7924.83	T-.9	18.62 ± 0.02	16.75 ± 0.02	15.85 ± 0.02	...	CS
Feb 04.33	7926.83	T-.9	...	16.84 ± 0.02	...	...	MMP
Feb 04.34	7926.84	T-.9	18.71 ± 0.03	...	...	...	MMP
Feb 08.34	7930.84	T-.9	18.82 ± 0.05	16.99 ± 0.02	16.16 ± 0.02	...	CS
Feb 10.35	7932.85	T-.9	18.69 ± 0.03	...	...	...	KE
Feb 10.37	7932.87	T-.9	18.63 ± 0.05	17.05 ± 0.02	16.20 ± 0.02	...	KE
Feb 12.35	7934.85	T-.9	18.77 ± 0.05	17.10 ± 0.02	16.28 ± 0.02	...	KE
Feb 15.32	7937.82	T-.9	18.85 ± 0.02	17.20 ± 0.02	16.38 ± 0.02	15.47 ± 0.02	LW/SH
Feb 16.32	7938.82	NTT	18.70 ± 0.05	17.18 ± 0.05	16.35 ± 0.03	...	MT
Feb 18.38	7940.88	T-.9	19.08 ± 0.03	17.25 ± 0.02	16.46 ± 0.02	...	OB
Feb 19.21	7941.71	T-.9	19.09 ± 0.03	17.31 ± 0.02	16.51 ± 0.02	...	OB
Feb 23.99	7946.48	A1.8	...	17.37 ± 0.06	16.63 ± 0.03	...	SB
Mar 05.29	7955.79	T-.9	19.22 ± 0.03	17.61 ± 0.02	...	...	AP
Mar 08.25	7958.75	NTT	...	...	17.00 ± 0.03	...	MT
Mar 09.26	7959.76	T-.9	19.35 ± 0.05	17.69 ± 0.02	...	...	AP
Mar 25.15	7975.65	T-4	...	...	...	16.50 ± 0.02	MN
Mar 25.16	7975.66	T-4	19.56 ± 0.03	18.05 ± 0.02	17.39 ± 0.02	...	MN
Apr 01.96	7983.44	A1.8	...	18.00 ± 0.08	17.56 ± 0.03	...	SB
Apr 03.20	7984.70	T-4	19.75 ± 0.14	18.47 ± 0.03	17.66 ± 0.05	16.83 ± 0.02	MN
Apr 17.17	7998.67	T-.9	19.96 ± 0.03	18.61 ± 0.03	17.85 ± 0.03	16.91 ± 0.02	MN
Apr 18.22	7999.72	E3.6	19.86 ± 0.08	...	17.76 ± 0.06	...	EC
May 02.13.....	8013.63	T-.9	20.22 ± 0.05	18.94 ± 0.02	18.16 ± 0.02	17.22 ± 0.02	LW
May 14.12.....	8025.62	T-.9	20.31 ± 0.07	19.25 ± 0.03	18.35 ± 0.02	17.47 ± 0.02	LW
May 28.24.....	8039.74	F-.6	...	19.51 ± 0.02	...	...	BL
May 28.26.....	8039.76	F-.6	...	...	18.45 ± 0.05	...	BL
Jun 01.16.....	8043.66	F-.6	...	...	...	17.75 ± 0.02	BL
Jun 01.18.....	8043.68	F-.6	...	...	18.66 ± 0.07	...	BL
Jan 15.42	8271.92	K-2	...	...	...	21.17 ± 0.08	BL
Jan 15.46	8271.96	K-2	...	...	22.85 ± 0.07	...	BL
Jan 15.46	8271.97	K-2	...	24.62 ± 0.34	...	...	BL

[a] JD − 2,440,000.

[b] Telescope key as follows: A1.8 = OAA 1.82 m; E3.6 = ESO 3.6 m; F-.6 = FLWO 0.61 m; K-2 = KPNO 2.1 m; NTT = ESO-NTT 3.5 m. T-.9 = CTIO 0.91 m; T-4 = CTIO 4.0 m.

[c] Observer key as follows. AP = A. Phillips; BL = B. Leibundgut; CS = C. Sturch; EC = E. Cappellaro; JT = J. A. Tyson; KE = K. Eastwood; LW = L. Wells; MMP = M. M. Phillips; MN = M. Navarrete; MP = M. Perez; MT = M. Turatto; PG = P. Guhathakurta; SB = S. Benetti; SH = S. Heathcote.

limits on the real slope. In order to get unbiased results, the background of the region where the SN appeared should be modeled using an image of the parent galaxy without the SN; this model should be subtracted from the images of the galaxy with the SN, and the photometric measurements should be made on the images with the background subtracted.

4. PHOTOMETRIC EVOLUTION

4.1. $BV(RI)_c$ Light Curves

The resulting light curves of SN 1990B are shown in Figure 8, where it is possible to see that SN 1990B belongs to the group of slow SESNe. SN 1990B is, hence, a slow Type Ic SNe (Clocchiatti et al. 1997; Clocchiatti & Wheeler 1997a, 1997b). It is also clear that maximum light was missed.

The well-observed light curve of SN 1993J (Richmond et al. 1994), a prototype SESN, can be used to give estimates of both the time of maximum and the foreground extinction. As shown in Figure 9, fitting the V light curve of SN 1993J to the postmaximum decay of SN 1990B indicates that its maximum light in V occurred on JD = 2,447,911, 2 days before discovery. The fit also implies that V maximum was $\sim$15.75 mag. Simultaneous fitting of the B and V light curves requires an additional shift to the red of the B light curve of SN 1993J, in the amount of $\sim$0.6 mag, as well as a shift to the blue of the R light curve of SN 1993J, in the amount of $\sim$0.1 mag, indicating that the foreground extinction of SN 1990B was appreciably larger than that of SN 1993J. The V light curve provides a good fit for some 40 days after V maximum, while a simultaneous fitting of the B and R bands is not as good. The trend seems to be that, soon after maximum, SN 1990B was brighter than SN 1993J in the red, while the colors became more similar in the early exponential tail.

Both the red color and the narrow Na D lines observed in the spectra indicate that SN 1990B was heavily reddened by foreground material in NGC 4568. The color excess of SN 1993J, measured by different techniques, was $E(B-V) = 0.25$ mag (Clocchiatti et al. 1995). The additional shift required to match the light curves implies that the color excess of SN 1990B was $E(B-V) \sim 0.85$ mag, if the intrinsic colors of SN 1990B and SN 1993J were the same. This estimate of the color excess is consistent with that of Suntzeff et al. (1990). The narrow Na I D lines measured in the spectra with the best S/N (7.5 ± 0.2 and 1.3 ± 0.2 Å) can be used to give another estimate of the foreground reddening. The equivalent width of the Na I D lines correlates with $E(B-V)$ although the correlation is both noisy and still very uncertain (see as examples Filippenko, Matheson, & Ho 1993 or Richmond et al. 1994). Usage of this correlation with the constant found by Clocchiatti et al. (1995) provides $E(B-V) \sim 1.76$ mag, an estimate consistent with that of Bennetti, Cappellaro, & Turatto (1990). Both estimates, although uncertain, give a range of values that probably bracket the correct foreground extinction toward SN 1990B.

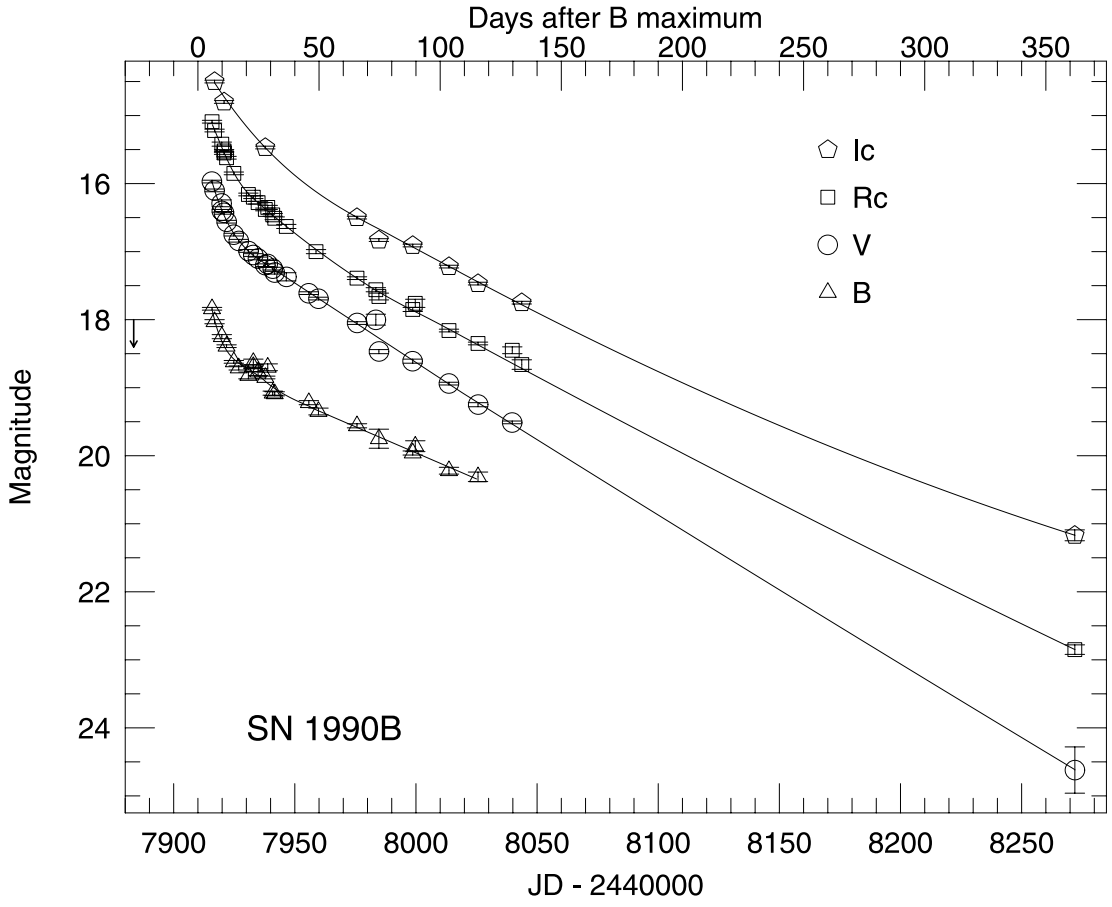

FIG. 8.—B, V, and R_c, I_c light curves of SN 1990B. The solid lines are the low-order polynomial fits used to build the $BV(RI)_c$ light curves (see § 4.2).

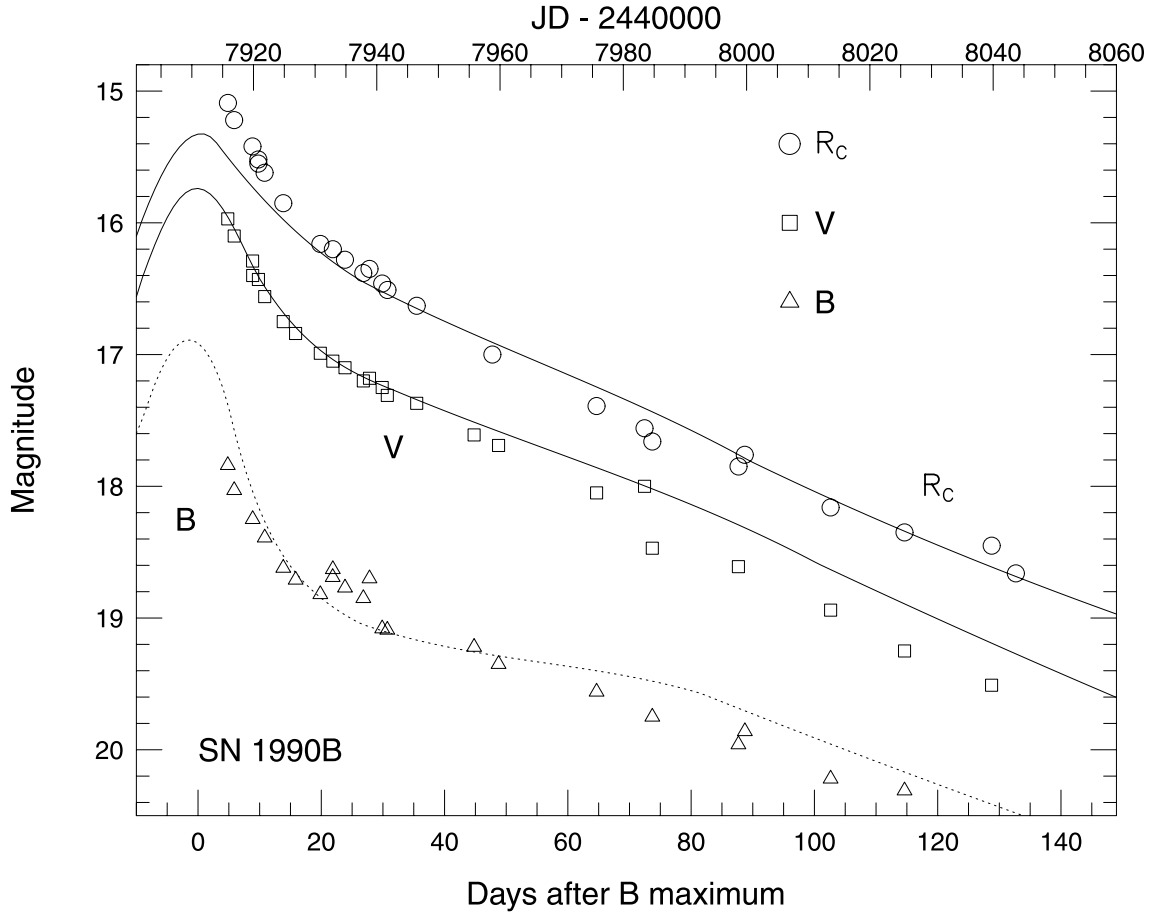

FIG. 9.—Comparison of the light curves of SN 1990B with those of SN 1993J (Richmond et al. 1994). The V light curve was fitted first, and differential vertical shifts were applied to the B and R_c light curves to account for differences in the foreground extinction (see § 4.1).

The postmaximum decay of SN 1990B is similar to that of SN 1993J. At $\sim$40 days after maximum, however, the B and V light curves start to deviate. The V light curve of SN 1990B enters a linear decay with a slope of $\sim$0.020 mag day^{-1}, while that of SN 1993J was $\sim$0.019 mag day^{-1}. The B light curve of SN 1990B enters a linear decay with a slope of $\sim$0.020 mag day^{-1}, while SN 1993J decayed at the slower rate of $\sim$0.019 mag day^{-1}. SN 1993J reaches the slope of SN 1990B only after a rather abrupt change $\sim$80 days after V maximum.

4.2. *OIR Light Curves*

The multicolor photometry of SN 1990B allows us to build optical-infrared (OIR) light curves to compare with theoretical models. Bolometric and OIR light curves are scarce. In order to progress with analysis and comparison, it has been customarily assumed that, soon after maximum light, the V light curves become parallel to the bolometric ones and can be used instead to know the speed of bolometric decay. This assumption can be tested in the case of SN 1990B.

We fitted the B, V, R_c, and I_c light curves with piecewise low-degree polynomials. Using the zero points of Bessell (1990), we converted the magnitudes of these fits into monochromatic flux densities at the filter effective wavelength, corrected the flux by foreground reddening using the galactic reddening law of Cardelli, Clayton, & Mathis (1989) for our two different estimates of $E(B-V)$, and integrated the flux densities using a simple trapezoidal rule.

The OIR light curves of SN 1990B are plotted in Figure 10, where we see that the V light curves are, indeed, a good representation of the OIR ones for most of the time of interest. Fitting straight lines to the late-time OIR light curves gives an asymptotic rate of decay for SN 1990B of 0.0195 ± 0.0005 or 0.0188 ± 0.003 for $A_V = 2.64$ or $A_V = 5.46$, respectively. The OIR light curve of SN 1990B approximately follows the track of the expanding spherical shell with a characteristic time for the decay of the opacity to γ-rays of $t_0 = 87$ days (Clocchiatti & Wheeler 1997b). SN 1993J falls on the track of the shell with $t_0 = 116$ days. If the explosion energy were the same for both SNe, then the expanding shell of SN 1990B would be smaller than that of 1993J by a factor of $\sim$0.75.

Comparison with the light curve of a Type Ic SN of the fast variety is also instructive. With this purpose, we have included in Figure 10 the OIR light curve of SN 1994I (Richmond et al. 1996). Relatively soon after maximum light, this is approximately 60 days in the case of SN 1994, the OIR light curve of a fast Type Ic SN reaches the asymptotic regime where the rate of decay in excess of the ^{56}Co decay rate is given by $\sim 2.2/t$, where t is the time since explosion (Clocchiatti & Wheeler 1997b). In a logarithmic

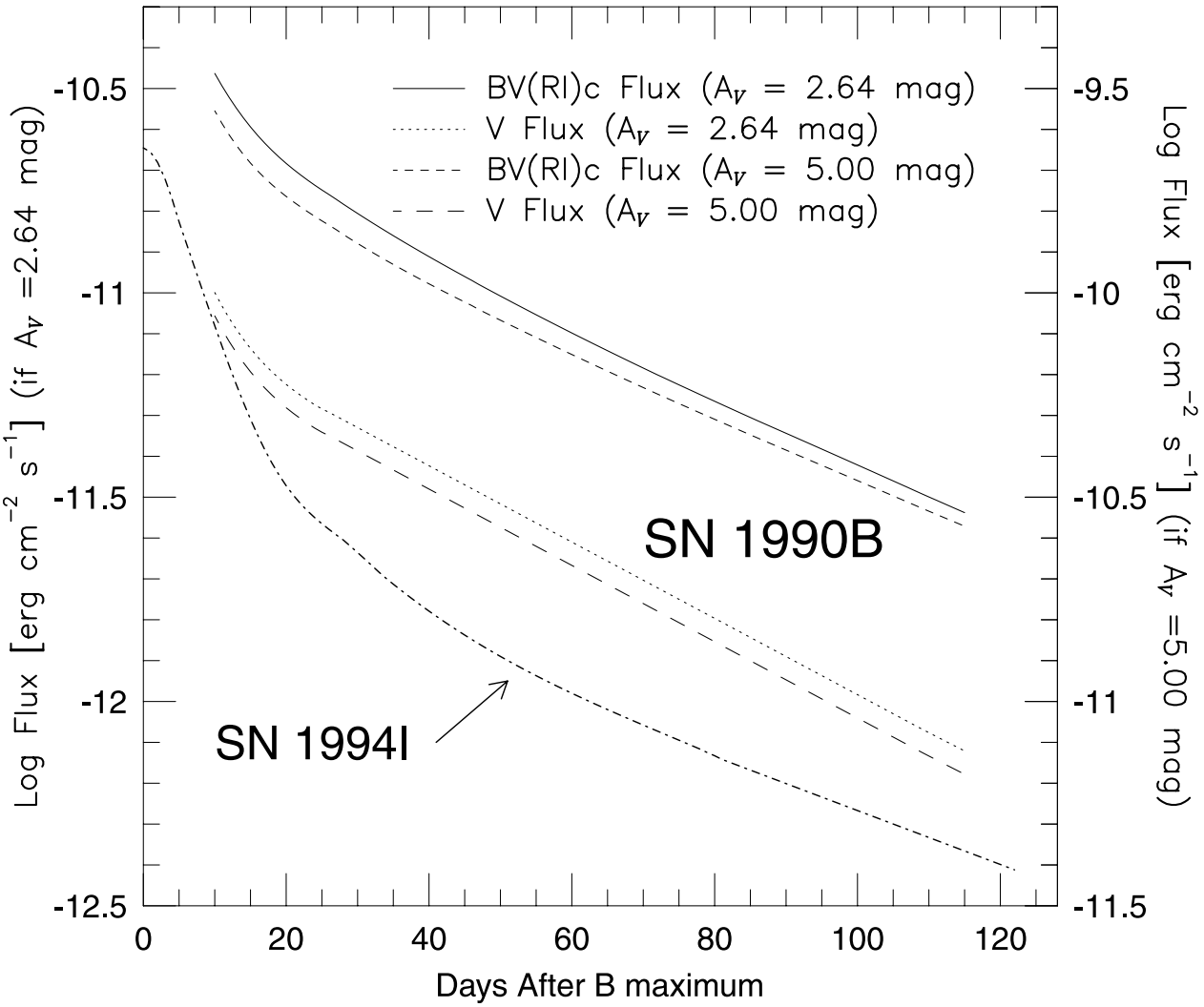

FIG. 10.—OIR light curves of SN 1990B (see § 4.2). Two different sets corresponding to different estimates of the foreground extinction are given. Note that, in order to make the figure more compact, two different vertical scales that span the same range are given. The OIR light curve of the fast Type Ic SN 1994I (Richmond et al. 1996) is also given.

plot like that of Figure 10, this behavior appears as a flattening of the light curve that develop a distinct positive curvature. Because of its slower rate of decay, SN 1990B does not enter the asymptotic regime for the ~120 days after maximum that our observations last.

5. DISCUSSION

SN 1990B is an example of a Type Ic SNe with an extensive set of well-sampled observations. The spectra sequence and light curves presented in the previous sections will permit detailed comparison with theoretical models and in depth comparative analysis with other well-observed SNe.

The extensive database of photometry allowed us to perform a test on the performance of two different techniques commonly used to measure the brightness of point-like sources. We found that, as the SN gets dimmer and the contrast between SN and parent galaxy background diminishes, usage of standard PSF fitting photometry results in an overestimate of the SN brightness and a related underestimate of the slope of the light-curve decay rate at late times. The same sort of effect was also found by Sollerman, Leibundgut, & Spyromilio (1998), in the study of the late-time light curve of SN 1996N. In the case of SNe, which given enough time do fade beyond detectability, the problem is solved by taking a very late time image and using it to model, and subtract, the background light.

SN 1990B was discovered soon after maximum light. The date of maximum found by comparison with SN 1993J, JD = 2,447,911, is essentially the same suggested by Van Dyk et al. (1993; JD = 2,447,910). If SN 1990B corresponds to a configuration similar to that of SN 1993J, then the very detailed studies of the latter would permit an estimate of the time of shock breakout of the former. Fitting the evolution of the angular radius of the photosphere of SN 1993J during the first 4 days of evolution, Clocchiatti et al. (1995) obtained shock breakout for SN 1993J on JD = 2,449,074.6. The maximum light in V for this SN took place on JD = 2,449,095 (Richmond et al. 1994), 20.4 days later. Shock breakout for SN 1990B should have occurred on JD ~ 2,447,891. This estimate is consistent with the negative observation by the Berkeley Automated SN Search on JD = 2,447,884, which was, hence, 5 days before shock breakout. Fitting simple models to the radio light curves of SN 1990B, Van Dyk et al. (1993) estimate the time of origin for the SN expansion as JD = 2,447,876, 35 days before maximum in B and 15 days before our estimated time of

shock breakout. Consideration of the uncertainties involved in the fits ($\sim$2 days in fitting the light curves and a few days in the case of the radio curves) indicates that the estimates can be considered marginally consistent.

The fact that the SN was heavily reddened complicates the analysis. Comparison with the light curves of other Type Ic SNe (Suntzeff et al. 1990) or SN 1993J (this paper) provides $E(B-V) \sim 0.85$, while the equivalent width of Na I D lines caused by foreground interstellar matter indicates a color excess a factor of 2 larger. Detailed model of the early spectra could provide an estimate of the intrinsic color of the SN and, hence, a better handle on the foreground extinction.

The Galactic foreground extinction in the direction of SN 1990B amounts to $E(B-V) \sim 0.033$ (Schlegel et al. 1998), while the narrow Na I D lines at the velocity of the interstellar matter in the Galaxy (an equivalent width of 1.3 ± 0.2 Å) seem to imply a larger $E(B-V)$. It is not possible to establish whether this is just another example of the large scatter in the correlation between $E(B-V)$ and the equivalent width of the Na I D lines in the Galaxy or an example of unresolved small-scale substructure in the Galactic reddening maps of Schlegel et al. (1998).

Fitting the V light curve of SN 1993J to that of SN 1990B allows us to estimate $V_{\max} \sim 15.75$ for the latter. The distance to NGC 4568 is not well known. Assuming it is at the distance of the Virgo Cluster, however, permits us to estimate an absolute V magnitude for SN 1990B. Taking $D_{\rm Virgo} = 15.9 \pm 2$ Mpc (Graham et al. 1999), one gets $M_V = -17.9$ or $M_V = -20.7$ for $A_V = 2.64$ or $A_V = 5.46$, respectively. The latter, more luminous, value is difficult to believe for a Type Ic SN, and especially for one that did not show particularly high expansion velocities. We take it as an indication that the largest estimate of foreground extinction is probably too high. The former, although less luminous, could appear as too bright for a core-collapse SN. Consideration of the cases of luminous Type Ic SNe such as SN 1992ar (Clocchiatti et al. 2000a) or SN 1998bw (Galama et al. 1998), which were brighter than our estimates for SN 1990B, makes it appear more reasonable. Van Dyk et al. (1993) propose that SN 1990B could correspond to a white dwarf and red supergiant star pair, with the white dwarf exploding very much like a Type Ia SN, after a period of mass accretion. The brightness estimates given above are consistent with this rather controversial view of a Type Ic SN.

Even though the evidence is indirect, we are convinced that SN 1990B carried small amounts of He in its outer expanding layers. The relative behavior of the Fe II and Na I D lines indicates so. The velocity of the He I layer, in spite of being poorly determined, seems to be considerably smaller than those on other Type Ic SNe (see Fig. 13 in Clocchiatti et al. 1997). It is, however, similar to the He I velocity in the Type II transition SN 1993J (Swartz et al. 1993). The absolute velocity of the lines, which is fairly directly related to the energy that the explosion deposits in the ejecta, can be very different for different SNe. The velocity contrast between the He I lines and lines of other elements (particularly Fe II and Na I D) would seem to carry an important piece of information regarding the progenitor structure. For objects that show little differences in early-time spectra, the velocity of the He I lines, their time evolution, and their velocity contrast with other ions might give us a handle of how to differentiate SNe coming from different progenitor stars. The difficulty in observing the optical He I lines, however, indicates that progress in this area will strongly depend on well-sampled infrared spectroscopy.

We thank the referee, S. D. Van Dyk, whose detailed comments greatly improved the paper. Support for A. C., at different stages of this project, was provided by P. Universidad Católica de Chile under DIPUC Project 97/12E and by FONDECYT, Chile, under Project 1980803. N. B. S. and M. M. P. acknowledge the support from NASA through grants GO-2563.01-87A and GO-6020 from STScI. This work is based partly on observations obtained at the Cerro Tololo Inter-American Observatory and Kitt Peak National Observatory, divisions of the National Optical Astronomy Observatories, which is operated by the Association of Universities for Research in Astronomy (AURA), Inc., under cooperative agreement with the National Science Foundation. This work is based partly on observations obtained at the European Southern Observatory, La Silla, Chile.

REFERENCES

Benetti, S., Cappellaro, E., & Turatto, M. 1990, IAU Circ. 4967
Bessell, M. S. 1990, PASP, 102, 1181
Cardelli, J. A., Clayton, G. C., & Mathis, J. S. 1989, ApJ, 345, 245
Clocchiatti, A., et al. 1995, ApJ, 446, 167
———. 1996, ApJ, 462, 462
———. 1997, ApJ, 483, 675
Clocchiatti, A. 2000a, BAAS, 197, 17.05
———. 2000b, ApJ, 529, 661
Clocchiatti, A., & Wheeler, J. C. 1997a, in Thermonuclear Supernovae, ed. P. Ruiz-Lapuente, R. Canal, & J. Isern (Dordrecht: Kluwer), 863
———. 1997b, ApJ, 491, 375
Cousins, A. W. J. 1976a, MmRAS, 81, 25
———. 1976b, Mon. Notes Astron. Soc. South Africa, 35, 70
———. 1978, Mon. Notes Astron. Soc. South Africa, 37, 8
de Vaucouleurs, G., de Vaucouleurs, A., Corwin, H. G., Jr., Buta, R. J., Paturel, G., & Fouqué, P. 1991, Third Reference Catalogue of Bright Galaxies (New York: Springer)
Dopita, M. A., & Ryder, S. D. 1990, IAU Circ. 4953
Filippenko, A. V. 1997, ARA&A, 35, 309
Filippenko, A. V., et al. 1995, ApJ, 450, L11
Filippenko, A. V., Matheson, T., & Ho, L. C. 1993, ApJ, 415, L103
Filippenko, A. V., Porter, A. C., & Sargent, W. L. W. 1990a, AJ, 100, 1575
Filippenko, A. V., Spinrad, H., & Dickinson, M. 1990b, IAU Circ., 4953
Galama, T. J., et al. 1998, Nature, 395, 670
Graham, J. A. 1982, PASP, 94, 244
Graham, J. A. 1999, ApJ, 516, 626
Johnson, H. L. 1955, Ann. d'Astrophys., 18, 292
Kirshner, R. P., Leibundgut B., & Horine, E. 1990, IAU Circ. 4953
Landolt, A. U. 1992, AJ, 104, 340
Menzies, J. W., Cousins, A. W. J., Banfield, R. M., & Laing, J. D. 1989, South African Astron. Obs. Circ., 13, 1
Panagia, N., Cassatella, A., Gonzalez-Riestra, R., Talavera, A., & Wamsteker, W. 1990, IAU Circ. 4959
Perlmutter, S., & Pennypacker, C. 1990, IAU Circ. 4949
Phillips, A. C., & Davis, L. E. 1995, in ASP Conf. Ser. 77, Astrophysical Data Analysis Software and Systems IV, ed. R. A. Shaw, H. E. Payne, & J. J. E. Hayes (San Francisco: ASP), 297
Richmond, M. W., et al. 1994, AJ, 107, 1022
———. 1996, AJ, 111, 327
Schlegel, D., Finkbeiner, D., & Davis, M. 1998, ApJ, 500, 525
Sollerman, J., Leibundgut, B., & Spyromilio, J. 1998, A&A, 337, 207
Sramek, R. A., Weiler, K. W., & Panagia, N. 1990, IAU Circ. 4979
Suntzeff, N., Perez, M., Wells, L., Phillips, M. M., & Ruiz, M.-T. 1990, IAU Circ. 4959
Swartz, D. A., Clocchiatti, A., Benjamin, R., Lester, D. F., & Wheeler, J. C. 1993, Nature, 365, 232
Van Dyk, S. D., Sramek, R. A., Weiler, K. W., & Panagia, N. 1993, ApJ, 409, 162
Wheeler, J. C., Harkness, R. P., Barker, E. S., Cochran, A. L., & Wills, D. 1987, ApJ, 313, L69